SIAM J. SCI. COMPUT.
Vol. 25, No. 6, pp. 2165–2187
© 2004 Society for Industrial and Applied Mathematics

Downloaded 07/08/12 to 147.8.148.246. Redistribution subject to SIAM license or copyright; see http://www.siam.org/journals/ojsa.php

# AN HLLC-TYPE APPROXIMATE RIEMANN SOLVER FOR IDEAL MAGNETOHYDRODYNAMICS*

K. F. GURSKI†

**Abstract.** This paper presents a solver based on the HLLC (Harten–Lax–van Leer contact wave) approximate nonlinear Riemann solver for gas dynamics for the ideal magnetohydrodynamics (MHD) equations written in conservation form. It is shown how this solver also can be considered a modification of Linde's "adequate" solver. This approximation method is intended to resolve slow, Alfvén, and contact waves better than the original HLL (Harten–Lax–van Leer) solver. Compared to exact nonlinear solvers and Roe's solver, this new solver is computationally inexpensive. In addition, the method will exactly resolve isolated contacts and fast shocks. The method also preserves positive density and pressure with two caveats: first, the numerical signal velocities (the eigenvalues of the Roe average matrix) do not underestimate the physical signal velocities, and second, in a very few cases it may be required to change the wavespeeds of the Riemann fan for the underlying HLL method to guarantee positive pressures. These conditions are less restrictive on the definitions of the wavespeeds than the conditions needed to make the HLLC method positively conservative for gas dynamics. While the method is intended for a three-dimensional MHD problem, the simulation results concentrate on one-dimensional test cases.

**Key words.** Riemann solver, magnetohydrodynamics, positivity

**AMS subject classifications.** 76W05, 85-08, 35L65, 65Z05

**DOI.** 10.1137/S1064827502407962

## 1. Introduction.

In the numerical simulation of ideal magnetohydrodynamics (MHD), just as with gas dynamics, there is an essential balance among capturing the key features of the flow, limiting computational expense, and maintaining robustness of the numerical method. High resolution requires a method with minimal numerical dissipation plus exact conservation of energy, mass, and momentum. Additionally, a physically real simulation requires that density and pressure remain positive under all circumstances and that a divergence-free magnetic field is preserved.

For gas dynamics, Einfeldt et al. [7] showed that the Godunov method [9] is a positively conservative differencing scheme that solves the Riemann problem. By definition of positively conservative, Godunov's scheme avoids nonphysical states with negative pressure and density while providing exact conservation of energy, mass, and momentum. One disadvantage of Godunov's method is the difficulty in solving the nonlinear Riemann problems for both gas dynamics and MHD. It has been argued that exact solutions are computationally expensive and involve a significant amount of detail that is actually irrelevant to solving numerical equations with Godunov's method. Hence, there is an interest in calculating approximate nonlinear Riemann solutions without expensive computations.

A natural first step for approximation might be towards a linearized Riemann solver. Roe [17] developed a difference scheme for gas dynamics based on the linearized Euler equations. However, Einfeldt et al. have demonstrated that for some choices of

*Received by the editors May 20, 2002; accepted for publication (in revised form) December 17, 2003; published electronically July 23, 2004. This work was partially performed while the author was employed by Universities Space Research Association at NASA Goddard Space Flight Center and was continued at the National Institute for Standards and Technology through support from the National Research Council Research Associateship Program.
http://www.siam.org/journals/sisc/25-6/40796.html
†Department of Mathematics, The George Washington University, Washington, D.C. 20052 (kgurski@gwu.edu).

Downloaded 07/08/12 to 147.8.148.246. Redistribution subject to SIAM license or copyright; see http://www.siam.org/journals/ojsa.php

initial data, Roe's difference scheme is unstable although a solution to the Riemann problem does exist. Einfeldt et al. also proved that for certain data any linearization will produce a negative density or pressure. Since ideal MHD can be reduced to the Euler equations by simply turning off the magnetic field, clearly a linearized Riemann solver for MHD will exhibit the same problems. Indeed, it has been shown that the Roe solver for MHD is computationally expensive and is not always well-behaved [3, 22, 15]. Recently several groups have proposed new "Roe-averages" for the MHD Roe solver that lead to a more stable solution, albeit at considerable computational expense [19, 16, 12].

In gas dynamics, a class of nonlinear Riemann solvers devised by Harten, Lax, and van Leer [11] has proved to be reliable, robust, and computationally inexpensive. The original Harten–Lax–van Leer (HLL) scheme assumes there is one average state between the two acoustic waves that bound the Riemann fan. Einfeldt et al. argued that the solver is positively conservative, an argument that Batten et al. [2] and Einfeldt et al. [7] noted is valid only when the wavespeeds used for the outer waves bound the Riemann fan.

Since the one average state HLL scheme is unable to resolve any contact waves, modifications to the basic HLL scheme were necessary. Einfeldt et al. [6, 7] offered a solution by replacing the intermediate HLL state with a linear state. With the constants suitably defined by Einfeldt et al., this HLLEM scheme gave an exact solution of an isolated contact discontinuity. Harten, Lax, and van Leer suggested that the single intermediate HLL constant state be replaced by a two intermediate state approximation was needed to capture the contact waves. Both Toro, Spruce, and Speares [21] and Batten et al. added the simplifications necessary that have defined the two-state HLL method for gas dynamics called the HLLC method. Batten et al. found the necessary conditions on the outermost acoustic wavespeeds to maintain positive pressure. While the HLLEM scheme has many virtues, this paper concentrates on the HLLC approach.

The HLL method has been generalized to MHD without computational difficulty and the gas dynamics HLL positivity proof can be extended to HLL for general MHD. Again positivity may require the enlargement of the Riemann fan by artificially moving the outermost waves at the expense of resolving shocks and expansions. As with gas dynamics, the MHD version of HLL suffers from the lack of contact, Alfvén, and slow wave information. The "adequate" method proposed by Linde [13] attempts to add this information within the HLL format; however, this method is not necessarily positively conservative and needs a new definition for one of the scalar variables.

In this paper we develop a new numerical method based on an extension of the gas dynamics HLLC solver to MHD. In addition to capturing the effects of contact waves, this HLLC method also resolves Alfvén and slow waves better than the HLL method. We will show how this method is similar to Linde's method and will use a similar smoothing device to remove oscillations while controlling positivity. Additionally, we include a short proof that this solver will exactly resolve isolated contacts and fast shocks. We also present a number of numerical examples, including comparisons with solutions to the HLL solver with all methods incorporating a first order Godunov scheme. These results are then compared with those from a Lax–Friedrichs solver shown on a fine spatial grid and with small timesteps to illustrate a convergence solution.

**2. Riemann problem and the Godunov flux for MHD.** We consider numerical methods for the solution of the ideal MHD equations—the limit in which

Downloaded 07/08/12 to 147.8.148.246. Redistribution subject to SIAM license or copyright; see http://www.siam.org/journals/ojsa.php

viscous and resistive effects are ignored—in conservation law form,

$$\int \Big[ U(\mathbf{x},t)_t dx - F(U(\mathbf{x},t))dt \Big] = 0, \quad U(\mathbf{x},0) = U_0(\mathbf{x},t), \tag{2.1}$$

and the vectors $U$ and $F$ are described in (2.2). Working in a coordinate system aligned locally with the flow, we consider $\mathbf{x}$ to be described by one spatial component normal to the flow, $x_n$, and two spatial components tangential to the flow, $x_{\tau_1}, x_{\tau_2}$. The state vector $U$ and flux $F$ are given by

$$U = \begin{pmatrix} \rho \\ \rho v_n \\ \rho v_{\tau_1} \\ \rho v_{\tau_2} \\ e \\ B_{\tau_1} \\ B_{\tau_2} \end{pmatrix}, \quad F = \begin{pmatrix} \rho v_n \\ \rho v_n^2 + p + \mathbf{B}^2/8\pi - B_n^2/4\pi \\ \rho v_{\tau_1} v_n - B_n B_{\tau_1}/4\pi \\ \rho v_{\tau_2} v_n - B_n B_{\tau_2}/4\pi \\ v_n(e + p + \mathbf{B}^2/8\pi) - (\mathbf{v}\cdot\mathbf{B})B_n/4\pi \\ B_{\tau_1} v_n - B_n v_{\tau_1} \\ B_{\tau_2} v_n - B_n v_{\tau_2} \end{pmatrix}, \tag{2.2}$$

where $\rho$, $e$, and $p$ represent the density, total energy per unit volume, and pressure, respectively. Similarly to the composition of the spatial vector $\mathbf{x}$, the velocity $\mathbf{v}$ and magnetic field $\mathbf{B}$ are broken into one component normal to the flow and two components tangential to the flow each. In the seven-wave MHD system, $B_n$ is assumed to be constant while the variables $B_{\tau_1}$ and $B_{\tau_2}$ satisfy the extra condition that $\nabla\cdot\mathbf{B} = 0$. Equation (2.1) illustrates the case where $\vec{n} = (1,0,0)^T$, but the results hold for arbitrary $\vec{n}$. In the general three-dimensional problem, one need only scale the flux per unit area by the interface area [2].

Restricting the problem to the one-dimensional Riemann problem with the flow normal in the $x$-direction, (2.1) then becomes

$$\begin{aligned} &U(x,t)_t + A_x U(x,t)_x = 0, \\ &U(x,0) = \begin{cases} U_L & \text{if} \quad x < 0, \\ U_R & \text{if} \quad x > 0, \end{cases} \end{aligned} \tag{2.3}$$

where the Jacobian matrix $A_x$ has the seven eigenvalues

$$\begin{aligned} \lambda_e &= v_n, && \text{an entropy wave,} \\ \lambda_a &= v_n \pm B_n/\sqrt{4\pi\rho}, && \text{a pair of Alfvén waves, and} \\ \lambda_{f,s} &= v_n \pm c_{f,s}, && \text{two pairs of magneto-acoustic waves.} \end{aligned}$$

The fast and slow magneto-acoustic speeds are given, respectively, by

$$c_{f,s} = \sqrt{\frac{1}{2}\left( \frac{\gamma p + \mathbf{B}\cdot\mathbf{B}/4\pi}{\rho} \pm \sqrt{\left( \frac{\gamma p + \mathbf{B}\cdot\mathbf{B}/4\pi}{\rho} \right)^2 - \frac{\gamma p B_n^2}{\pi\rho^2}} \right)}, \tag{2.4}$$

where $\gamma$ is the gas constant. Figure 1 shows the structure of the exact solution of the seven-wave Riemann problem for the specific case $\vec{n} = (1,0,0)^T$.

**3. The HLL solver.** The HLL Riemann solver was designed by Harten, Lax, and van Leer [11] as an approximate Riemann solver for the gas dynamics problem.

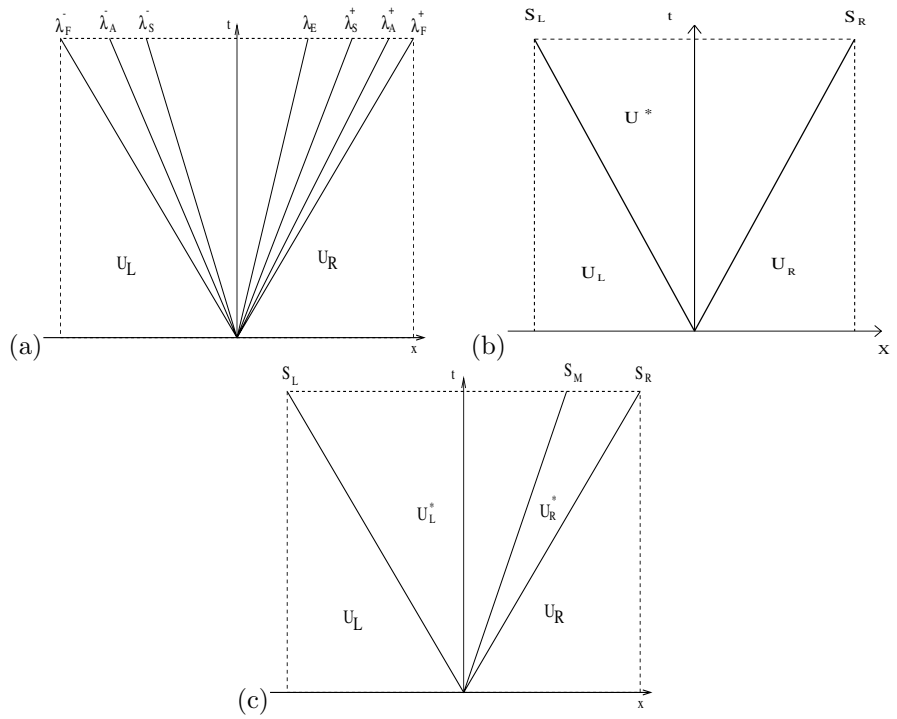


FIG. 1. (a) *Structure of the exact solution of the Riemann problem for the x-split three-dimensional MHD equations. There are seven wave families associated with the eigenvalues* $\lambda_F^-, \lambda_A^-, \lambda_S^-, \lambda_E, \lambda_S^+, \lambda_A^+, \lambda_F^+$. (b) *Structure of the solution of the HLL Riemann problem.* (c) *Structure of the solution of the HLLC Riemann problem.*

The HLL solver approximates the five-wave system with the two outermost acoustic waves (see [20, 2] for good summaries) and can be adapted without complications to the seven-wave MHD system shown in Figure 1. In both the gas dynamics and MHD cases there is a constant average state, $U^*$, between two waves of known speeds $S_L$ and $S_R$ as shown in Figure 1. In the MHD problem, the outermost waves are the fast magneto-acoustic waves. The choice for the wavespeeds $S_L$ and $S_R$ follow the wavespeed algorithm by Einfeldt et al. [7],

$$\begin{aligned} S_L &= \min[\lambda_1(U_L), \lambda_1(U^{Roe})], \\ S_R &= \max[\lambda_m(U_R), \lambda_m(U^{Roe})], \end{aligned} \tag{3.1}$$

where $\lambda_1(U^{Roe})$ and $\lambda_m(U^{Roe})$ are the smallest and largest eigenvalues of the Roe-averaged matrix. Correspondingly $\lambda_1(U_L)$ and $\lambda_m(U_R)$ are the smallest and largest eigenvalues of the left and right states of the matrix $A_x$. For MHD this becomes

$$\begin{aligned} S_L &= \min[v_{nL} - c_{F,L}, \hat{v}_n - \hat{c}], \\ S_R &= \max[v_{nR} + c_{F,R}, \hat{v}_n + \hat{c}], \end{aligned} \tag{3.2}$$

where $\hat{v}_n$ represents the Roe-averaged normal velocity and $\hat{c}$ the Roe-averaged fast magneto-acoustic wavespeed. Direct comparisons of different Roe-averaging techniques for the ideal MHD equations show that these Roe-averages are not unique. Linde uses the straightforward Brio–Wu Roe-averaging technique derived in [3] for

Downloaded 07/08/12 to 147.8.148.246. Redistribution subject to SIAM license or copyright; see http://www.siam.org/journals/ojsa.php

Downloaded 07/08/12 to 147.8.148.246. Redistribution subject to SIAM license or copyright; see http://www.siam.org/journals/ojsa.php

$\gamma = 2$, adapted for general $\gamma$ in [10, 14]. Other choices include the Roe-averages from Cargo and Gallice [4] and Balsara [1]. The numerical tests in this paper were performed with each of these three definitions for MHD Roe-averages and showed no significant difference in the results for the one-dimensional Brio–Wu [3] and Ryu–Jones [18] test problems. Note that the arithmetic-averaging method from the Ryu and Jones paper does not provide Roe-averages. This will be discussed further in section 4.1.

The HLL approximate Riemann state vector is defined as

$$U_{HLL} = \begin{cases} U_L & \text{if} \quad S_L > 0, \\ U^* & \text{if} \quad S_L \le 0 \le S_R, \\ U_R & \text{if} \quad S_R < 0, \end{cases} \tag{3.3}$$

where

$$U^* = \frac{S_R U_R - S_L U_L - F_R + F_L}{S_R - S_L}. \tag{3.4}$$

The Godunov-type flux is then represented as

$$F_{HLL} = \begin{cases} F_L & \text{if} \quad S_L > 0, \\ F^* & \text{if} \quad S_L \le 0 \le S_R, \\ F_R & \text{if} \quad S_R < 0, \end{cases} \tag{3.5}$$

where

$$F^* = \frac{S_R F_L - S_L F_R + S_L S_R (U_R - U_L)}{S_R - S_L}. \tag{3.6}$$

For gas dynamics, Davis [5] showed that the HLL Riemann solver satisfies the entropy inequality. In addition Harten, Lax, and van Leer showed that the gas dynamics HLL Riemann solver resolves isolated fast shocks exactly.

**3.1. Positivity of HLL scheme.** A Riemann solver is positively conservative if and only if all the states generated are physically real and the exact solution does not contain a vacuum state. The set of physically real MHD states is the set $G$ with positive densities and pressures:

$$G = \left\{ \begin{array}{l} (\rho, \rho v_n, \rho v_{\tau_1}, \rho v_{\tau_2}, e, B_{\tau_1}, B_{\tau_2})^T, \quad \text{where} \\ \rho > 0 \quad \text{and} \quad \phi = e - \frac{1}{2}\rho \mathbf{v}^2 - \frac{1}{8\pi}\mathbf{B}^2 > 0 \end{array} \right\}. \tag{3.7}$$

If both the scheme is positively conservative and the initial states are contained in $G$, then the generated states will be contained in $G$. The set $G$ can be reduced from MHD to gas dynamics by setting $\mathbf{B}$ to zero.

Einfeldt et al. argued that the HLL solver is positively conservative since the intermediate state $U^*$ is just an average of the two positive states $U_L$ and $U_R$. The argument hinges on two issues. First, the set $G$ must be convex, and second, the wavespeeds $S_L$ and $S_R$ must be bounded by the lower and upper bounds for the physical signal velocity, respectively.

The convexity of $G$ implies that for any states $U_1$ and $U_2$ both contained in $G$, $U = (1 - \lambda)U_1 + \lambda U_2$ is contained in $G$ for any $\lambda$ bounded between zero and one inclusively. The physical positivity conditions for the MHD version of the HLL center

Downloaded 07/08/12 to 147.8.148.246. Redistribution subject to SIAM license or copyright; see http://www.siam.org/journals/ojsa.php

state $U^*$ are

$$\rho^* = (1-\lambda)\rho_1 + \lambda\rho_2 > 0,$$
$$\phi^* = (1-\lambda)\phi_1 + \lambda\phi_2 + \frac{\lambda(\lambda-1)}{2}\left(\frac{\rho_1\rho_2}{\rho^*}(\Delta\mathbf{v})^2 + \frac{(\Delta\mathbf{B})^2}{4\pi}\right) > 0, \tag{3.8}$$

where the subscripts 1 and 2 could represent $R$ or $L$ interchangeably. Therefore if $U_L$ and $U_R$ are contained in $G$, then both $\rho^*$ and $\phi^*$ are positive. Therefore $U^*$ is contained in convex $G$.

Batten et al. identified a small problem in the second part of the Einfeldt et al. proof. The wavespeeds $S_L$ and $S_R$ as defined by (3.2) are not always the lower and upper bounds for the physical signal velocity. The inconsistencies can occur when multiple waves collide in or collapse from a single cell. Thus, it may be necessary to define $S_R$ larger or $S_L$ smaller to ensure positivity, a result suggested by the MHD simulations of Janhunen [12]. However, Davis [5] showed that the wavespeed algorithm given in (3.2) enforces the entropy condition at expansions and captures the resolution of Roe's approximate Riemann solver at shocks. By enlarging the Riemann fan by artificially placing the outermost waves beyond the fast magnetoacoustic waves, these benefits are lost. Batten et al. claimed that for gas dynamics the wavespeed algorithm of (3.2) had proven extremely robust. Likewise for MHD, it is not clear how often this wavespeed enlargement will be necessary; in the numerical simulations conducted by the author, neither $S_R$ nor $S_L$ needed to be redefined to maintain positive pressures.

**4. Extending the HLLC solver for gas dynamics to MHD.** While the HLL approximate Riemann solver exactly captures isolated fast shocks with the wavespeeds defined by (3.2), it smears the effects of isolated contact discontinuities. Harten, Lax, and van Leer's two-state HLL Riemann solver has been developed fully into the HLLC method, which accurately captures contact and shear waves for gas dynamics by the efforts of Toro, Spruce, and Speares [21] and Batten et al. [2]. In this section we present the results of directly applying the HLLC scheme to the seven-wave MHD problem.

In the HLLC approximate Riemann solver, the intermediate state $U^*$ is replaced with two averaged states $U_L^*$ and $U_R^*$ separated by a contact wave of speed $S_M$ as shown in Figure 1. The state vector and corresponding interface flux are then

$$U_{hllc} = \begin{cases} U_L & \text{if} \quad S_L > 0, \\ U_L^* & \text{if} \quad S_L \le 0 < S_M, \\ U_R^* & \text{if} \quad S_M \le 0 \le S_R, \\ U_R & \text{if} \quad S_R < 0, \end{cases} \qquad F_{hllc} = \begin{cases} F_L & \text{if} \quad S_L > 0, \\ F_L^* & \text{if} \quad S_L \le 0 < S_M, \\ F_R^* & \text{if} \quad S_M \le 0 \le S_R, \\ F_R & \text{if} \quad S_R < 0. \end{cases} \tag{4.1}$$

The wavespeeds $S_L$ and $S_R$ are defined as in (3.2). Applying the Rankine–Hugoniot conditions across the $S_L$, $S_M$, and $S_R$ waves gives

$$S_L U_L^* - F_L^* = S_L U_L - F_L, \tag{4.2}$$
$$S_M U_R^* - F_R^* = S_M U_L^* - F_L^*, \tag{4.3}$$
$$S_R U_R - F_R = S_R U_R^* - F_R^*. \tag{4.4}$$

The Rankine–Hugoniot conditions for the jump across the outermost waves may be

Downloaded 07/08/12 to 147.8.148.246. Redistribution subject to SIAM license or copyright; see http://www.siam.org/journals/ojsa.php

rewritten as

$$
\begin{aligned}
& S_i \begin{pmatrix} \rho_i^* \\ \rho_i^* v_{ni}^* \\ \rho_i^* v_{\tau_1 i}^* \\ \rho_i^* v_{\tau_2 i}^* \\ e_i^* \\ B_{\tau_1 i}^* \\ B_{\tau_2 i}^* \end{pmatrix} - \begin{pmatrix} \rho_i^* v_{ni}^* \\ \rho_i^* v_{ni}^{*2} + p_i^* + \mathbf{B}_i^{*2}/8\pi - B_n^2/4\pi \\ \rho_i^* v_{\tau_1 i}^* v_{ni}^* - B_n B_{\tau_1 i}^*/4\pi \\ \rho_i^* v_{\tau_2 i}^* v_{ni}^* - B_n B_{\tau_2 i}^*/4\pi \\ v_{ni}^*(e_i^* + p_i^* + \mathbf{B}_i^{*2}/8\pi) - B_n(\mathbf{B}_i^* \cdot \mathbf{v}_i^*)/4\pi \\ B_{\tau_1 i}^* v_{ni}^* - B_n v_{\tau 1 i}^* \\ B_{\tau_2 i}^* v_{ni}^* - B_n v_{\tau_2 i}^* \end{pmatrix} \\
& \quad = S_i \begin{pmatrix} \rho_i \\ \rho_i v_{ni} \\ \rho_i v_{\tau_1 i} \\ \rho_i v_{\tau_2 i} \\ e_i \\ B_{\tau_1 i} \\ B_{\tau_2 i} \end{pmatrix} - \begin{pmatrix} \rho_i v_{ni} \\ \rho_i v_{ni}^2 + p_i + \mathbf{B}_i^2/8\pi - B_n^2/4\pi \\ \rho_i v_{\tau_1 i} v_{ni} - B_n B_{\tau_1 i}/4\pi \\ \rho_i v_{\tau_2 i} v_{ni} - B_n B_{\tau_2 i}/4\pi \\ v_{ni}(e_i + p_i + \mathbf{B}_i^2/8\pi) - B_n(\mathbf{B}_i \cdot \mathbf{v}_i)/4\pi \\ B_{\tau_1 i} v_{ni} - B_n v_{\tau_1 i} \\ B_{\tau_2 i} v_{ni} - B_n v_{\tau_2 i} \end{pmatrix}. \qquad (4.5)
\end{aligned}
$$

First we derive the corresponding Godunov fluxes. Multiplying (4.2) by $S_R$ and subtracting (4.4) multiplied by $S_L$ gives

$$S_R S_L(U_R^* - U_L^*) - S_L F_R^* + S_R F_L^* = S_L S_R(U_R - U_L) - S_L F_R + S_R F_L. \qquad (4.6)$$

Using the definition for $F^*$ from (3.6) we can replace the right-hand side of (4.6) as follows:

$$S_R S_L(U_R^* - U_L^*) - S_L F_R^* + S_R F_L^* = (S_R - S_L)F^* \qquad \text{or} \qquad (4.7)$$

$$S_R F_L^* - S_L F_R^* = (S_R - S_L)F^* - S_L S_R \Delta U^*, \qquad (4.8)$$

where $F^*$ represents the single intermediate flux from the HLL method as defined in (3.6) and $\Delta U^* = U_R^* - U_L^*$. We then alternately replace $F_R^*$ and $F_L^*$ in (4.8) with the expression from (4.3) to obtain

$$F_L^* = F^* - \frac{S_L(S_R - S_M)}{(S_R - S_L)}\Delta U^*, \qquad (4.9)$$

$$F_R^* = F^* + \frac{S_R(S_M - S_L)}{(S_R - S_L)}\Delta U^*. \qquad (4.10)$$

Next, we must determine $U_R^*$ and $U_L^*$. We note that the Rankine–Hugoniot equations provide a zero jump in the velocity in the normal direction and in the total pressure (fluid pressure plus magnetic pressure) across a contact discontinuity [8]. Following the ideas behind the wavespeed estimate for the HLLC Riemann solver for gas dynamics as defined by Batten et al., we define

$$S_M = v_{nL}^* = v_{nR}^* = v_n^*, \qquad (4.11)$$

$$P^* = (p_L^* + \mathbf{B}_L^{*2}/8\pi) = (p_R^* + \mathbf{B}_R^{*2}/8\pi), \qquad (4.12)$$

where $v_n^*$ is the average normal velocity and $P^*$ is the total pressure between the two magneto-acoustic waves. Evaluating the Rankine–Hugoniot jump conditions for momentum in the normal direction from (4.2) and (4.4), one may write

$$S_L(\rho_L^* v_{nL}^* - \rho_L v_{nL}) - (F_{L2}^* - F_{L2}) = S_R(\rho_R^* v_{nR}^* - \rho_R v_{nR}) - (F_{R2}^* - F_{R2}),$$

Downloaded 07/08/12 to 147.8.148.246. Redistribution subject to SIAM license or copyright; see http://www.siam.org/journals/ojsa.php

where $F_{i2}$ represents the component of the flux corresponding to the normal momentum term in the $i$th direction. Since $v_{nL}^* = v_{nR}^* = S_M$, one can solve the above equation for $S_M$ to find

$$S_M = \frac{\rho_L v_{nL}(v_{nL} - S_L) - \rho_R v_{nR}(v_{nR} - S_R) + p_L - p_R + (\mathbf{B}_L^2 - \mathbf{B}_R^2)/8\pi}{\rho_L(v_{nL} - S_L) - \rho_R(v_{nR} - S_R)}. \tag{4.13}$$

This definition for $S_M$ is equivalent to $v_n^*$ from the HLL method. With $S_M$ defined, the other components of $U_L^*$ and $U_R^*$ may be defined in terms of $S_M$. Let $i = L, R$; then

$$\rho_i^* = \rho_i \frac{(S_i - v_{ni})}{(S_i - S_M)}, \tag{4.14}$$

$$P^* = p_i + \rho_i(v_{ni} - S_i)(v_{ni} - S_M) + \frac{\mathbf{B}_i^2}{8\pi}. \tag{4.15}$$

If the normal component of the magnetic field is nonzero, a contact discontinuity in MHD has only a density discontinuity, thereby requiring continuous tangential fluid velocities and magnetic field components [8]. This is a feature unique to MHD and does not pertain to gas dynamics. Consequently the following relationships for the tangential velocities and magnetic field components exist for $B_n \neq 0$:

$$\begin{aligned} v_{\tau_j L}^* &= v_{\tau_j R}^* = v_{\tau_j}^*, \\ B_{\tau_j L}^* &= B_{\tau_j R}^* = B_{\tau_j}^*, \quad \text{where} \quad j = 1, 2. \end{aligned} \tag{4.16}$$

Therefore, when $B_n \neq 0$ the equations for the energy and the tangential velocities and magnetic fields are replaced by

$$\begin{aligned} v_{\tau_j}^* &= \frac{\rho_L v_{\tau_j L}(v_{nL} - S_L) - \rho_R v_{\tau_j R}(v_{nR} - S_R)}{\rho_L(v_{nL} - S_L) - \rho_R(v_{nR} - S_R)} \\ &\quad + \frac{B_n(B_{\tau_j R} - B_{\tau_j L})/8\pi}{\rho_L(v_{nL} - S_L) - \rho_R(v_{nR} - S_R)}, \end{aligned} \tag{4.17}$$

$$B_{\tau_j}^* = \frac{B_{\tau_j L}(v_{nL} - S_L) - B_{\tau_j R}(v_{nR} - S_R) + B_n(v_{\tau_j R} - v_{\tau_j L})}{S_R - S_L}, \tag{4.18}$$

$$\begin{aligned} e_i^* &= \frac{\mathbf{B}_i^2 v_{ni}/2 + 4\pi\big(p_i v_{ni} + e_i(v_{ni} - S_i) - P^* S_M\big)}{4\pi(S_M - S_i)} \\ &\quad + \frac{B_n(\mathbf{B}_i^* \cdot \mathbf{v}_i^* - \mathbf{B}_i \cdot \mathbf{v}_i)}{4\pi(S_M - S_i)}. \end{aligned} \tag{4.19}$$

Similarly for $B_n = 0$,

$$v_{\tau_j i}^* = v_{\tau_j i}, \tag{4.20}$$

$$B_{\tau_j i}^* = \frac{B_{\tau_j i}(S_i - v_{ni})}{(S_i - S_M)}, \tag{4.21}$$

$$e_i^* = \frac{\mathbf{B}_i^2 v_{ni}/2 + 4\pi\big(p_i v_{ni} + e_i(v_{ni} - S_i) - P^* S_M\big)}{4\pi(S_M - S_i)}. \tag{4.22}$$

There is one problem with this formulation. One can see that for nonzero $B_n$ the tangential velocities and magnetic fields are identical to those given by the HLL method. While this formulation captures the sharpness of the contact discontinuity

Downloaded 07/08/12 to 147.8.148.246. Redistribution subject to SIAM license or copyright; see http://www.siam.org/journals/ojsa.php

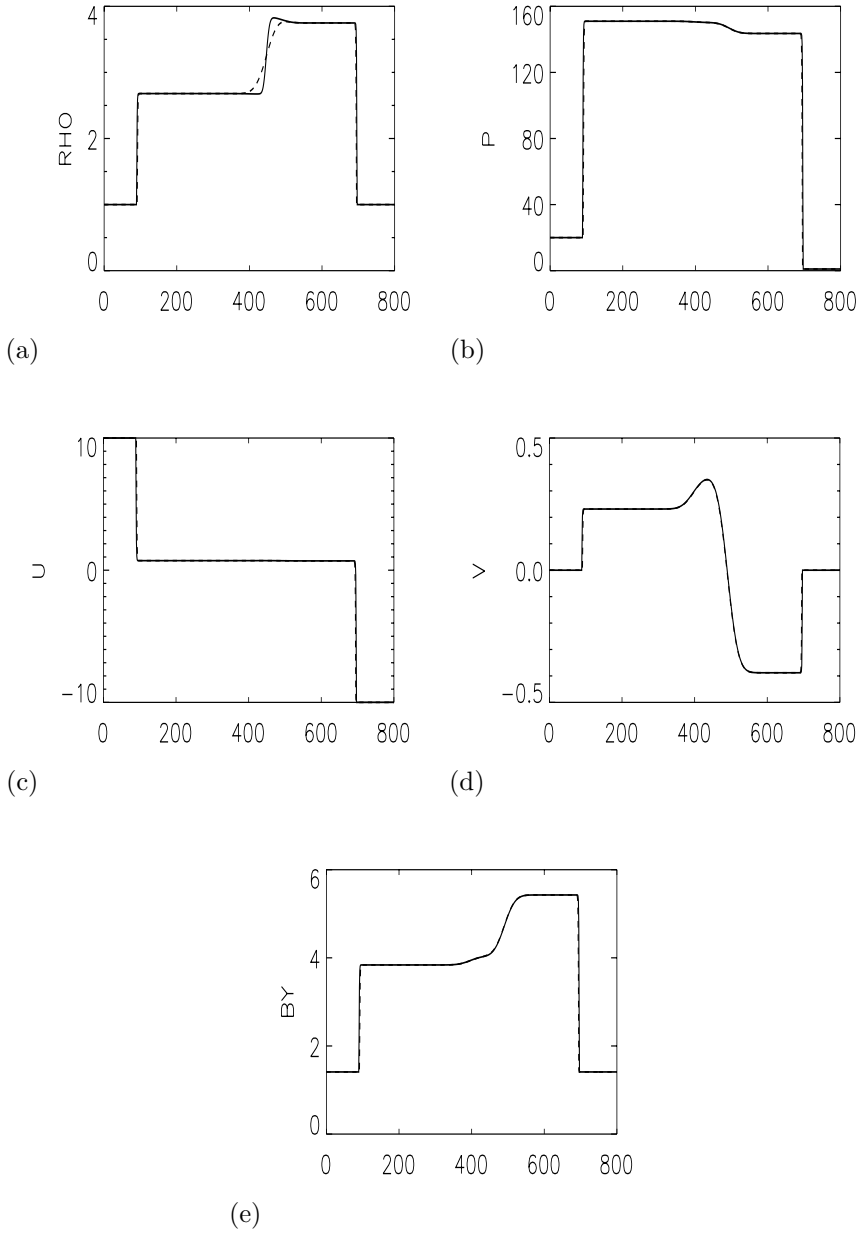


FIG. 2. *Comparison of the HLL method with the HLLC method for MHD with the* $B_n \neq 0$ *jump conditions. Test problem shown is Ryu–Jones problem* 1a [18] *with* $\gamma = 5/3$, $CFL = 0.8$, *and* 800 *cells. The* $B_n \neq 0$ *jump conditions version of HLLC were used for the solid curve. The dashed curve corresponds to the HLL method.*

(manifested only by a jump in density), there is no benefit gained for the tangential velocities and magnetic fields for the slow and Alfvén waves in using this formulation over the HLL method. This effect is illustrated by the results for the MHD shock tube test of Ryu and Jones [18] in Figure 2. In this numerical simulation the normal direction is in the $x$-direction; therefore $v_n = u$, $v_{\tau_1} = v$, $v_{\tau_2} = w$, $B_n = B_x$, $B_{\tau_1} = B_y$,

Downloaded 07/08/12 to 147.8.148.246. Redistribution subject to SIAM license or copyright; see http://www.siam.org/journals/ojsa.php

TABLE 1
*One-dimensional MHD test problems.*

| Test | $\rho$ | $P$ | $u$ | $v$ | $w$ | $B_x$ | $B_y$ | $B_z$ | $t_s$ |
|---|---|---|---|---|---|---|---|---|---|
| RJ left | 1 | 20 | 10 | 0 | 0 | 5 | 5 | 0 | 0.08 |
| RJ right | 1 | 1 | $-10$ | 0 | 0 | 5 | 5 | 0 | |
| BW left | 1 | 1 | 0 | 0 | 0 | 0.75 | 1 | 0 | 0.8 |
| BW right | 0.125 | 0.1 | 0 | 0 | 0 | 0.75 | $-1$ | 0 | |
| T left | 1 | 1000 | $-19.59745$ | 0 | 0 | 1 | 1 | 0 | 0.12 |
| T right | 1 | 0.01 | $-19.59745$ | 0 | 0 | 1 | 1 | 0 | |

and $B_{\tau_2} = B_z$. The initial left and right states are given in Table 1. In this scheme $\gamma = 5/3$, the Courant–Friedrichs–Lewy (CFL) number $= 0.8$, the $x$-interval is divided into 800 cells, and the initial discontinuity is placed in the center of the interval. From left to right the plots show a fast shock, a slow rarefaction, a contact discontinuity, a slow shock, and a fast shock. In this figure, the dashed curve corresponds to the HLL method. The solid curve corresponds to the HLLC method described above, using (4.17)–(4.22), that recognizes the continuity in the tangential velocities and magnetic fields across the contact discontinuity. Unfortunately, neither method captures the slow waves. For comparison the Lax–Friedrichs convergence solution with 20,000 cells and 40,000 timesteps is shown in Figure 3.

The success of numerical solvers is typically measured in the improvement in calculating the density, and this method clearly restores the contact wave in the density calculation. However, we believe that it is possible to restore the jumps in the other quantities in the slow and Alfvén waves within the HLLC framework.

The HLLC method approximates the full seven-wave Riemann system with just three waves. If the additional four waves were added to the system, the extra conditions of (4.16) would not result in a reduction of the method to HLL in the tangential velocity and magnetic field components. To avoid this reduction in our approximate system, we choose not to explicitly incorporate continuity in tangential velocity and magnetic fields across the discontinuity for nonzero $B_n$. In the instances where the discontinuity is a slow or Alfvén wave, these primitive quantities would not necessarily be continuous. Since we are attempting to maintain the compatibility with the gas dynamics HLLC solver in the zero normal magnetic field limit, we will retain the continuity of the normal velocity and total pressure across the middle wave. The corresponding definitions for the tangential velocity and magnetic field follow from (4.2)–(4.4). One can see that these definitions will satisfy the previously stated relations for $B_n = 0$.

$$v^*_{\tau_j i} = \frac{B_{\tau_j i} B_n (S_M - v_{ni})}{B_n^2 + 4\pi\rho_i (v_{ni} - S_i)(S_i - S_M)} + v_{\tau_j i}, \tag{4.23}$$

$$B^*_{\tau_j i} = \frac{B_{\tau_j i}\big(B_n^2 - 4\pi\rho_i (v_{ni} - S_i)^2\big)}{B_n^2 + 4\pi\rho_i (v_{ni} - S_i)(S_i - S_M)}. \tag{4.24}$$

The equations for $v^*_{ni}$, $\rho^*_i$, and $e^*_i$ for arbitrary $B_n$ are given by (4.13), (4.14), and (4.19), respectively. The corresponding $U^*_L$ and $U^*_R$ defined by (4.13), (4.14), (4.19), (4.23), (4.24) do not satisfy the Rankine–Hugoniot condition, and this unphysical

Downloaded 07/08/12 to 147.8.148.246. Redistribution subject to SIAM license or copyright; see http://www.siam.org/journals/ojsa.php

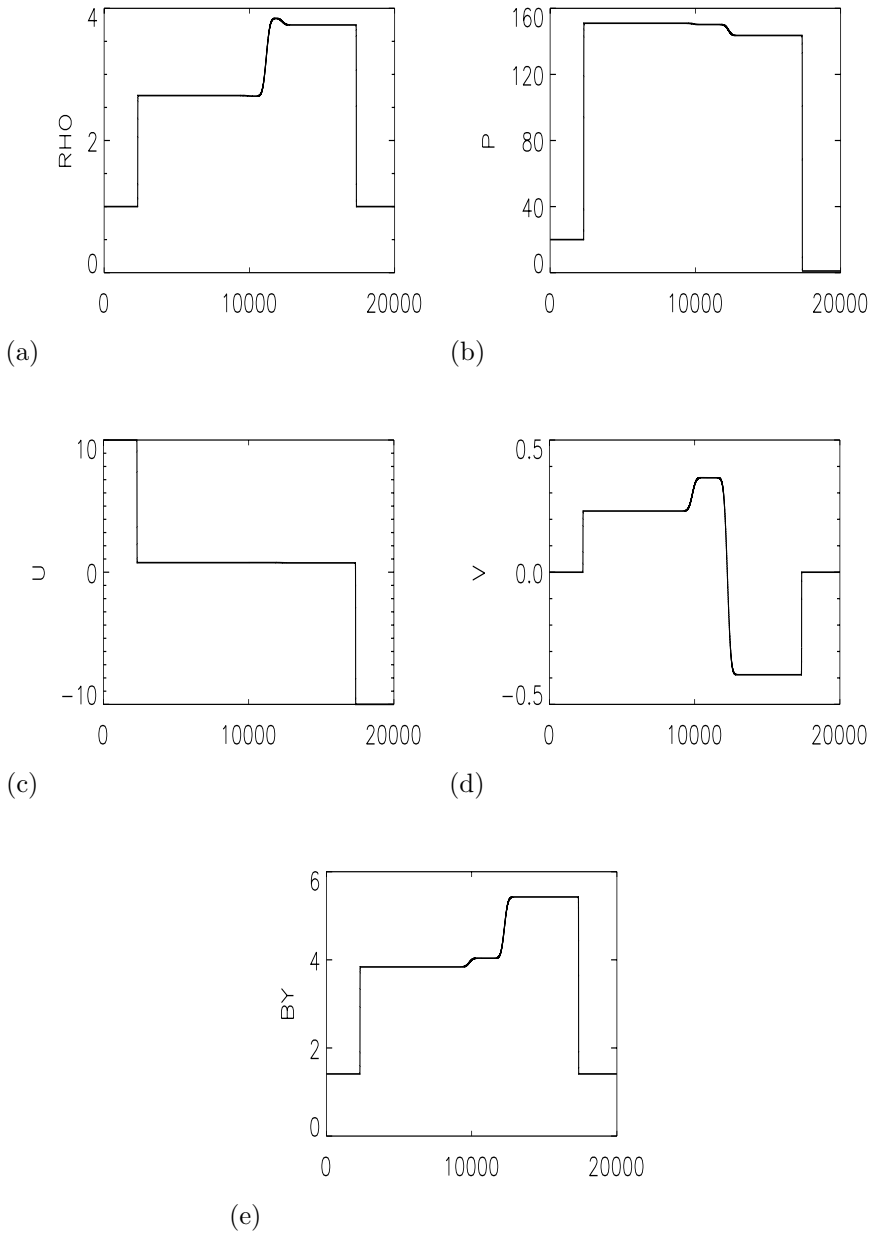


FIG. 3. *Lax–Friedrichs scheme for the Ryu–Jones test problem* 1a *with* $\gamma = 5/3$, 20,000 *cells, and* 40,000 *timesteps.*

choice may cause oscillations. When this new method is applied to the Ryu–Jones test problem, the sharpness along the slow waves is restored to the tangential velocity and magnetic field components as shown in Figure 4. However, this formulation does introduce some oscillations away from the contact discontinuity as seen in the Brio–Wu [3] test, shown in Figure 5. The initial left and right states are given in Table 1. In this scheme $\gamma = 2$, CFL $= 0.8$, the $x$-interval is divided into 800 cells, and the initial

Downloaded 07/08/12 to 147.8.148.246. Redistribution subject to SIAM license or copyright; see http://www.siam.org/journals/ojsa.php

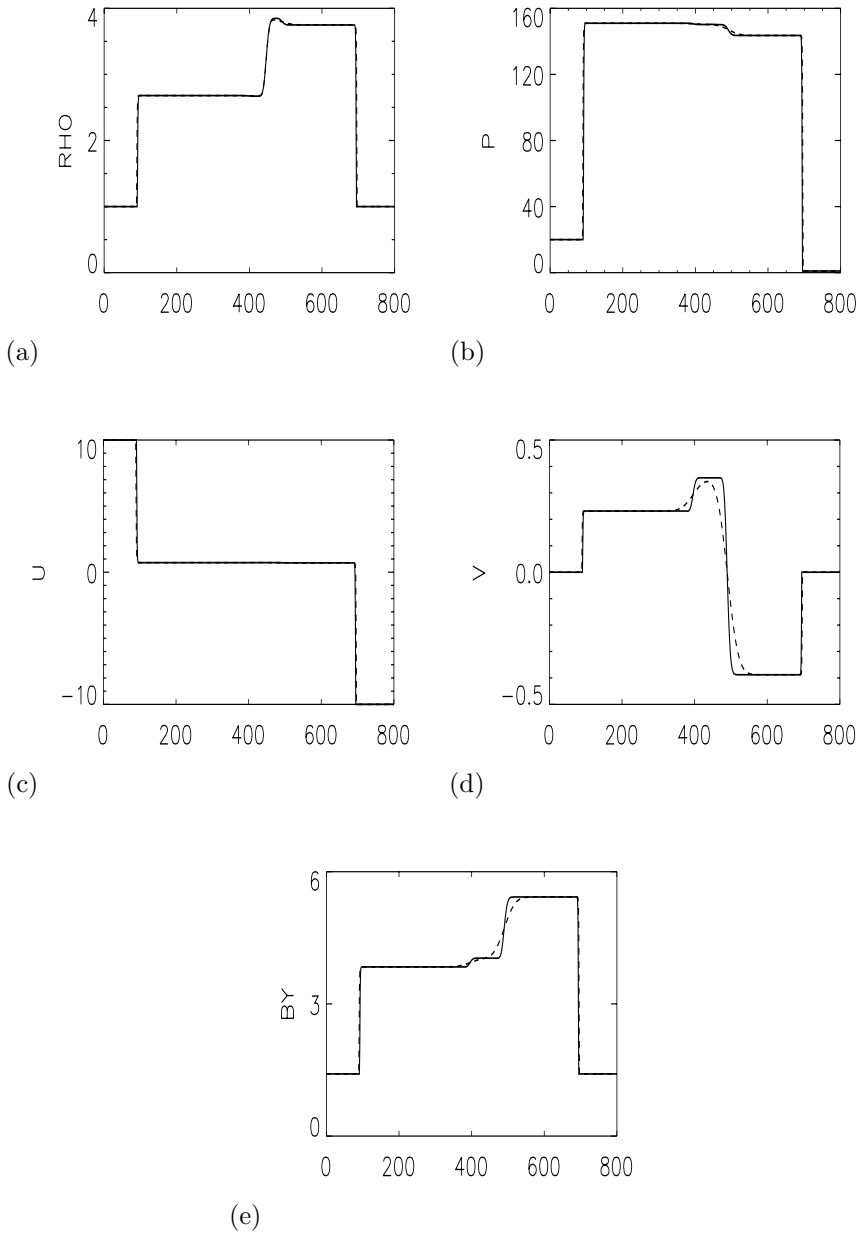


FIG. 4. *Comparison of the two HLLC methods for MHD. Test problem shown is Ryu–Jones problem* 1a [18] *with* $\gamma = 5/3$, *CFL* $= 0.8$, *and* 800 *cells. The* $B_n \neq 0$ *jump conditions version of HLLC were used for the dashed curve. The solid curve represents the HLLC method without those extra conditions.*

discontinuity is placed in the center of the interval. The plots show a fast rarefaction and a slow compound wave moving to the left. The plots have a contact discontinuity, a slow shock, and a fast rarefaction moving to the right.

In section 6 we present a smoothed version of the HLLC for MHD in which a small amount of dissipation is added to control these unwanted oscillations.

Downloaded 07/08/12 to 147.8.148.246. Redistribution subject to SIAM license or copyright; see http://www.siam.org/journals/ojsa.php

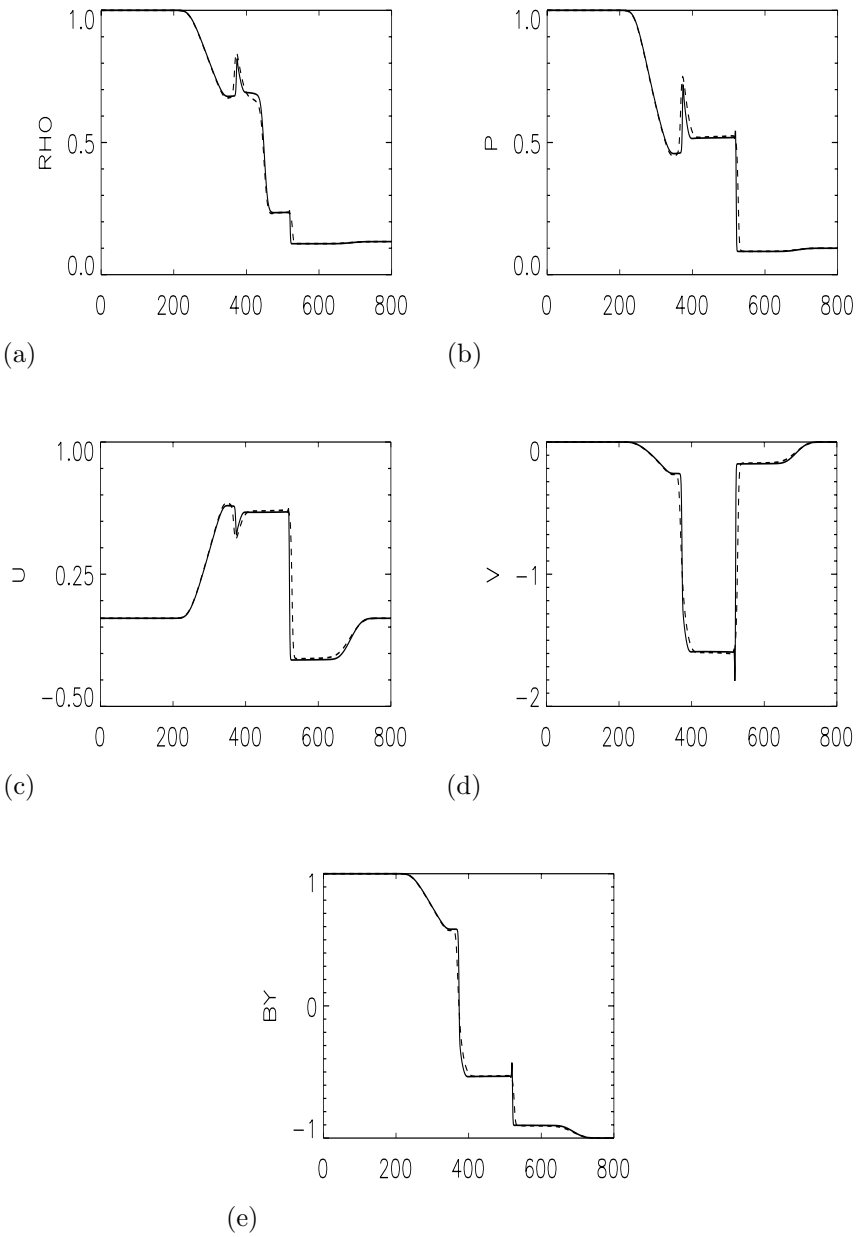


FIG. 5. *Two versions of extending the HLLC method for MHD. Test problem shown is Brio–Wu* [3] *with* $\gamma = 2$, *CFL* $= 0.8$, *and* 800 *cells. The* $B_n \neq 0$ *jump conditions were used for the dashed curve.*

**4.1. Positivity of MHD-HLLC scheme.** For the MHD problem, $\rho_L^*$ and $\rho_R^*$ as defined in (4.14) will be positive if and only if $S_L < S_M < S_R$ when $S_L < 0 < S_R$. If an arithmetic average [18] is used in place of a Roe-averaged wavespeed in (3.1), this property will not always hold because the outer wavespeeds may still underestimate the physical signal speeds. For example, consider the test case of a virtually stationary

Downloaded 07/08/12 to 147.8.148.246. Redistribution subject to SIAM license or copyright; see http://www.siam.org/journals/ojsa.php

contact wave from Toro's [20] gas dynamics example with a magnetic field added. In this instance the tangential discontinuity splits into a slow wave, a contact wave, and another slow wave. (See Table 1 for initial states with $\gamma = 1.4$.) Since the magnetic field is weak compared to the pressure, the three waves travel at different but nearly equal speeds, and using an arithmetic average with (3.1) provides an underestimate of the magnitude of $S_L$ and $S_R$. However, (3.1) used with the Roe-averages defined by either Cargo and Gallice [4] or Balsara [1] avoids this problem in part by incorporating Alfvén wavespeed averages rather than a straight magnetic field average (among other differences).

Considering the left-star state for pressure and positivity requires

$$\phi_L^* = e_L^* - \frac{1}{2}\rho_L^* \mathbf{v_L^*}^2 - \frac{1}{8\pi}\mathbf{B_L^*}^2 > 0. \tag{4.25}$$

First we substitute in the definitions for $e_L^*$, $\mathbf{v_L^*}$, and $\mathbf{B_L^*}$ from the previous section. Next we substitute $e_L = p_L/(\gamma-1)+\rho_L \mathbf{v_L}^2/2+\mathbf{B}_L^2/4\pi$. For notational ease we define $S_M - v_{nL} = \zeta$, $v_{nL} - S_L = \eta$ and note that $\eta > 0$ and $\zeta + \eta = S_M - S_L > 0$. Then (4.25) for nonzero $B_n$ (the case $B_n = 0$ is discussed later in this section) becomes (after much algebraic manipulation)

$$\begin{aligned} 2(\gamma-1)(\zeta+\eta)\phi_L^* = {} & \frac{\zeta^2(\gamma-1)\eta\rho_L \mathbf{B}_{LT}^2/4\pi}{B_n^2/4\pi - \rho_L\eta(\zeta+\eta)} \\ & + \zeta^2(\gamma-1)\rho_L\eta - 2\zeta(\gamma-1)p_L + 2p_L\eta, \end{aligned} \tag{4.26}$$

where $\mathbf{B}_{LT}^2 = \mathbf{B}_L^2 - B_n^2$. The first term in (4.26) is bounded with a more manageable term, resulting in the following inequality:

$$\begin{aligned} 2(\gamma-1)(\zeta+\eta)\phi_L^* > {} & \frac{\zeta^2(\gamma-1)\eta\rho_L \mathbf{B}_{LT}^2}{B_n^2} \\ & + \zeta^2(\gamma-1)\rho_L\eta - 2\zeta(\gamma-1)p_L + 2p_L\eta. \end{aligned} \tag{4.27}$$

Requiring the right-hand side of (4.27) to be positive is a stronger condition than requiring (4.25) to be valid. For arbitrary $\zeta$

$$\begin{aligned} & 4(\gamma-1)p_L\left((\gamma-1)p_L - 2\frac{\mathbf{B}_L^2}{B_n^2}\eta^2\rho_L\right) < 0 \qquad \text{or} \\ & S_L < v_{nL} - \sqrt{\frac{(\gamma-1)p_L B_n^2}{2\mathbf{B}_L^2\rho_L}}. \end{aligned} \tag{4.28}$$

When $B_n = 0$, (4.26) is replaced by

$$\begin{aligned} 2(\gamma-1)(\zeta+\eta)\phi_L^* = {} & \zeta^2(\gamma-1)\eta\rho_L + 2p_L\Big(\eta + (\gamma-1)\zeta\Big) \\ & - \frac{\zeta^2(\gamma-1)\mathbf{B}_{LT}^2/4\pi}{(\zeta+\eta)}. \end{aligned} \tag{4.29}$$

Since $\zeta^2(\gamma-1)\mathbf{B}_{LT}^2/4\pi > 0$ and $\zeta+\eta > 0$, we can choose to enforce the more stringent

Downloaded 07/08/12 to 147.8.148.246. Redistribution subject to SIAM license or copyright; see http://www.siam.org/journals/ojsa.php

condition that

$$2(\gamma-1)(\zeta+\eta)\phi_L^* > \zeta^2(\gamma-1)\eta\rho_L + 2p_L\Big(\eta+(\gamma-1)\zeta\Big) > 0.$$

This requires, for arbitrary $\zeta$,

$$4(\gamma-1)p_L\Big((\gamma-1)p_L - 2\rho_L\eta^2\Big) < 0 \qquad \text{or}$$

$$S_L < v_{nL} - \sqrt{\frac{(\gamma-1)p_L}{2\rho_L}}. \tag{4.30}$$

This result is identical to the positivity condition found by Batten et al. [2] for the gas dynamics HLLC scheme.

A similar proof for the right-star state for pressure provides the necessary restrictions on $S_R$ to guarantee positivity. Thus we find that in order to preserve positivity for the HLLC-MHD method we must enlarge the Riemann fan by altering the wavespeeds of $S_L$ and $S_R$. We find below in section 6.1 that our device for damping the oscillations in the solution also will allow a means to control positivity without altering $S_L$ and $S_R$ except for a very few cases.

**4.2. Exact resolution of isolated contacts and fast shocks for HLLC-MHD solver.** The following section shows that the HLLC-MHD solver will resolve exactly isolated contact discontinuities and shocks. This resolution is controlled by the definition of the middle wavespeed, $S_M$, and the definition of $U_L^*$ and $U_R^*$.

An isolated contact discontinuity has

$$\begin{aligned} v_{nL} &= v_{nR} = v_n, \\ p_L + \mathbf{B}_L^2/4\pi &= p_R + \mathbf{B}_R^2/4\pi. \end{aligned} \tag{4.31}$$

Substituting (4.31) into (4.13) gives $S_M = v_n$. From (4.1) we obtain the exact solution for general $x/t$,

$$U = \begin{cases} U_L & \text{if} \quad x/t < v_n, \\ U_R & \text{if} \quad x/t > v_n, \end{cases} \tag{4.32}$$

which holds for any choice of $S_L$ and $S_R$.

The shock velocity $S$ of an isolated fast shock is given by the largest (or smallest) eigenvalue of the Roe matrix [17]. Without loss of generalization, assume that $S_R = S$. Then the Rankine–Hugoniot jump conditions are

$$\begin{aligned} S(\rho_L - \rho_R) &= \rho_L v_{nL} - \rho_R v_{nR}, \\ S(\rho_L v_{nL} - \rho_R v_{nR}) &= \rho_L v_{nL}^2 + P_L - \frac{B_n^2}{4\pi} - \left(\rho_R v_{nR}^2 + P_R - \frac{B_n^2}{4\pi}\right), \\ S(\rho_L v_{\tau_j L} - \rho_R v_{\tau_j R}) &= \rho_L v_{\tau_j L} v_{nL} - \frac{B_n B_{\tau_j L}}{4\pi} - \left(\rho_R v_{\tau_j R} - \frac{B_n B_{\tau_j R}}{4\pi}\right), \\ S(e_L - e_R) &= v_{nL}(e_L + P_L) - (\mathbf{v}_L \cdot \mathbf{B}_L)\frac{B_n}{4\pi} \\ &\quad - \left(v_{nR}(e_R + P_R) - (\mathbf{v}_R \cdot \mathbf{B}_R)\frac{B_n}{4\pi}\right), \\ S(B_{\tau_j L} - B_{\tau_j R}) &= B_{\tau_j L} v_{nL} - B_n v_{\tau_j L} - (B_{\tau_j R} v_{nR} - B_n v_{\tau_j R}). \end{aligned} \tag{4.33}$$

Downloaded 07/08/12 to 147.8.148.246. Redistribution subject to SIAM license or copyright; see http://www.siam.org/journals/ojsa.php

Substituting the first two equations from (4.33) into (4.13) gives $S_M = v_{nL}$. Using this definition with (4.14), (4.19), (4.23), (4.24), and (4.33) also gives $U_L^* = U_L$ for a shock connected with the $S_R$ wave. With much algebraic manipulation we also find that $U_R^* = U_L^*$.

When the shock is connected with the $S_L$ wave, the appropriate Rankine–Hugoniot jump conditions show that $U_L^* = U_R^* = U_R$. For an isolated fast shock wave, these relations simplify to

$$U = \begin{cases} U_L & \text{if} \quad x/t < S, \\ U_R & \text{if} \quad x/t > S. \end{cases} \tag{4.34}$$

**5. Linde's "adequate" solver.** The three-wave MHD "adequate" solver developed by Linde [13] attempts to restore the contact discontinuity information to the HLL solver through a different technique from the HLLC-MHD solver described above.

Linde noted that if the middle wave is the isolated discontinuity, the jump across the middle wave is equal to $U_R - U_L$. Otherwise, the jump across the middle wave is zero. These two cases are captured by the relationship

$$U_R^* - U_L^* = \alpha(U_R - U_L), \quad \alpha \in [0, 1], \tag{5.1}$$

for a scalar $\alpha$ where the outer and intermediate states are defined as dimensionless quantities. By substituting (5.1) into (4.2) and (4.4), the following alternate expressions for the intermediate state vectors and fluxes are obtained:

$$U_L^* = U_L + \frac{(1-\alpha)S_R + \alpha\hat{v}_n}{S_R - S_L}\Delta U - \frac{1}{S_R - S_L}\Delta F, \tag{5.2}$$

$$U_R^* = U_R + \frac{(1-\alpha)S_L + \alpha\hat{v}_n}{S_R - S_L}\Delta U - \frac{1}{S_R - S_L}\Delta F, \tag{5.3}$$

$$F_L^* = \frac{S_L((1-\alpha)S_R + \alpha\hat{v}_n)}{S_R - S_L}\Delta U - \frac{S_L}{S_R - S_L}F_R + \frac{S_R}{S_R - S_L}F_L, \tag{5.4}$$

$$F_R^* = \frac{S_R((1-\alpha)S_L + \alpha\hat{v}_n)}{S_R - S_L}\Delta U - \frac{S_L}{S_R - S_L}F_R + \frac{S_R}{S_R - S_L}F_L, \tag{5.5}$$

where $\Delta U = U_R - U_L$, $\Delta F = F_R - F_L$, and $\hat{v}_n$ is a generalization of the Brio–Wu (originally defined for $\gamma = 2$) Roe-averaged normal wavespeed.

The scalar $\alpha$ is defined using the $L_1$ vector norm,

$$\alpha_{Linde} = \max[0, 1 - s], \tag{5.6}$$

$$\text{where} \quad s = \frac{\|\Delta F - \hat{v}_n \Delta U\|}{\hat{c}\|\Delta U\|}, \tag{5.7}$$

for the appropriately dimensionless $U$ and $F$. The quantity $\hat{c}$ is the Brio–Wu Roe-averaged fast magneto-acoustic speed.

Downloaded 07/08/12 to 147.8.148.246. Redistribution subject to SIAM license or copyright; see http://www.siam.org/journals/ojsa.php

Linde's method restores the missing contact, slow, and Alfvén waves to the HLL method for MHD and therefore returns a less diffusive solution than HLL. What is lacking in this simple scheme is a true scalar definition for $\alpha$ and a means to control positivity.

**6. Smooth HLLC-type solver for MHD.** We note that the flux in Linde's method given by (5.4)–(5.5) can be written as

$$F_L^* = F^* - \alpha \frac{S_L(S_R - \hat{v}_n)}{(S_R - S_L)} \Delta U, \tag{6.1}$$

$$F_R^* = F^* + \alpha \frac{S_R(\hat{v}_n - S_L)}{(S_R - S_L)} \Delta U. \tag{6.2}$$

If $\Delta U^* = \alpha \Delta U$ and $\hat{v}_n = S_M$, then (6.1)–(6.2) are identical to the flux equations (4.9)–(4.10) for the HLLC-MHD solver. Thus, we see that combining (6.1)–(6.2) with our definitions of the intermediate $U_L^*$ and $U_R^*$ states will smooth the unwanted oscillations that occur when we do not assume that the tangential velocities and magnetic fields are continuous across the contact discontinuity. There are two issues to resolve: the normalization of $\alpha$ and a control of positivity.

In this section we specify a normalization technique to justify Linde's scalar $\alpha$. Additionally we will present an easy algorithm for maintaining positive pressures in the simulation.

We define the vectors $\Delta W$ and $\Delta W^*$,

$$\Delta W = \begin{pmatrix} S\Delta\rho \\ \Delta(\rho v_n) \\ \Delta(\rho v_{\tau_1}) \\ \Delta(\rho v_{\tau_2}) \\ \Delta(\sqrt{\rho e}) \\ \Delta(\sqrt{\rho} B_{\tau_1}) \\ \Delta(\sqrt{\rho} B_{\tau_2}) \end{pmatrix} \quad \text{and} \quad \Delta W_* = \begin{pmatrix} S\Delta\rho^* \\ S_M\Delta\rho^* \\ \Delta(\rho^* v_{\tau_1}^*) \\ \Delta(\rho^* v_{\tau_2}^*) \\ \Delta(\sqrt{\rho^* e^*}) \\ \Delta(\sqrt{\rho^*} B_{\tau_1}^*) \\ \Delta(\sqrt{\rho^*} B_{\tau_2}^*) \end{pmatrix}, \tag{6.3}$$

where

$$S \equiv \begin{cases} S_M & \text{if} \quad S_M \neq 0, \\ \min(|S_L|, |S_R|) & \text{if} \quad S_M = 0. \end{cases}$$

Next we can define the matrices $A$ and $A_*$,

$$A = \begin{pmatrix} S & 0 & 0 & 0 & 0 & 0 & 0 \\ 0 & 1 & 0 & 0 & 0 & 0 & 0 \\ 0 & 0 & 1 & 0 & 0 & 0 & 0 \\ 0 & 0 & 0 & 1 & 0 & 0 & 0 \\ \overline{\sqrt{e}}\delta & 0 & 0 & 0 & \overline{\sqrt{\rho}}/(2\overline{\sqrt{e}}) & 0 & 0 \\ \overline{B_{\tau_1}}\delta & 0 & 0 & 0 & 0 & \overline{\sqrt{\rho}} & 0 \\ \overline{B_{\tau_2}}\delta & 0 & 0 & 0 & 0 & 0 & \overline{\sqrt{\rho}} \end{pmatrix}, \tag{6.4}$$

Downloaded 07/08/12 to 147.8.148.246. Redistribution subject to SIAM license or copyright; see http://www.siam.org/journals/ojsa.php

$$A_* = \begin{pmatrix} S & 0 & 0 & 0 & 0 & 0 & 0 \\ 0 & 1 & 0 & 0 & 0 & 0 & 0 \\ 0 & 0 & 1 & 0 & 0 & 0 & 0 \\ 0 & 0 & 0 & 1 & 0 & 0 & 0 \\ \overline{\sqrt{e^*}}\delta^* & 0 & 0 & 0 & \overline{\sqrt{\rho^*}}/(2\overline{\sqrt{e^*}}) & 0 & 0 \\ \overline{B^*_{\tau_1}}\delta^* & 0 & 0 & 0 & 0 & \overline{\sqrt{\rho^*}} & 0 \\ \overline{B^*_{\tau_2}}\delta^* & 0 & 0 & 0 & 0 & 0 & \overline{\sqrt{\rho^*}} \end{pmatrix}, \tag{6.5}$$

where $\overline{q} = (q_R + q_L)/2$, $\delta = (2\overline{\sqrt{\rho}})^{-1}$, and $\delta^* = (2\overline{\sqrt{\rho^*}})^{-1}$. Then as $A\Delta U = \Delta W$ and $A_*\Delta U^* = \Delta W_*$, where $\Delta U$ and $\Delta U^*$ are as defined previously, (5.1) may be replaced by

$$\begin{aligned} A_*^{-1}\Delta W_* &= \alpha A^{-1}\Delta W, \\ (AA_*^{-1}\Delta W_*)^T(\Delta W) &= \alpha(\Delta W)^T\Delta W, \\ (AA_*^{-1}\Delta W_*)^T(\Delta W)/\|\Delta W\| &= \alpha, \end{aligned} \tag{6.6}$$

where the norm is defined as the $L_2$ vector norm.

Our second change to Linde's solver is to replace the use of the Roe-averaged wavespeed $\hat{v}_n$ with the middle wavespeed $S_M$. Lastly, we choose to forego any smoothing in the first component of $U_i^*$ and $F_i^*$. This will allow changes in the density along the contact discontinuity to remain unsmoothed and will allow a control of positivity. In this instance

$$U_i^*(1) = \rho_i^*, \tag{6.7}$$

$$U_i^*(k) = U^*(k) + \alpha\frac{S_M - S_i}{S_R - S_L}\Delta U, \tag{6.8}$$

$$F_i^*(1) = \rho_i^* S_M, \tag{6.9}$$

$$F_L^*(k) = F^*(k) - \alpha\frac{S_L(S_R - S_M)}{(S_R - S_L)}\Delta U(k), \tag{6.10}$$

$$F_R^*(k) = F^*(k) + \alpha\frac{S_R(S_M - S_L)}{(S_R - S_L)}\Delta U(k), \tag{6.11}$$

where $\rho_i^*$ is as defined in the HLLC-MHD solver in (4.14), $\alpha$ is defined in (6.6), $U^*$ is the intermediate HLL state, $F^*$ is the intermediate HLL flux, $i = L, R$, and $k = 2, 3, 4, 5, 6, 7$.

When this smoothed HLLC-MHD method is applied to the Ryu–Jones 1a test problem, the results are nearly identical to those for the unsmoothed HLLC-MHD method. In fact, these results are plotted in Figure 4, with a dashed curve, but the results are indistinguishable from the nonsmoothed HLLC-MHD method shown with the solid curve. In addition, in comparison to the previous results for the Brio–Wu test problem shown in Figures 5–6, Figure 7 illustrates that the smooth HLLC-MHD adds sufficient dissipation to remove the oscillations without losing additional sharpness.

**6.1. Positivity of smooth HLLC-MHD scheme.** The decision to remove the $\alpha$-smoothing from the first component of $U_i^*$ and $F_i^*$ allows a means to assure that the scheme preserves positivity. Clearly the densities $\rho_L^*$ and $\rho_R^*$ will remain positive for appropriately defined $S_L$ and $S_R$ as was discussed in section 4.1. It remains to check the conditions on the pressure in the left-star and right-star regions.

Downloaded 07/08/12 to 147.8.148.246. Redistribution subject to SIAM license or copyright; see http://www.siam.org/journals/ojsa.php

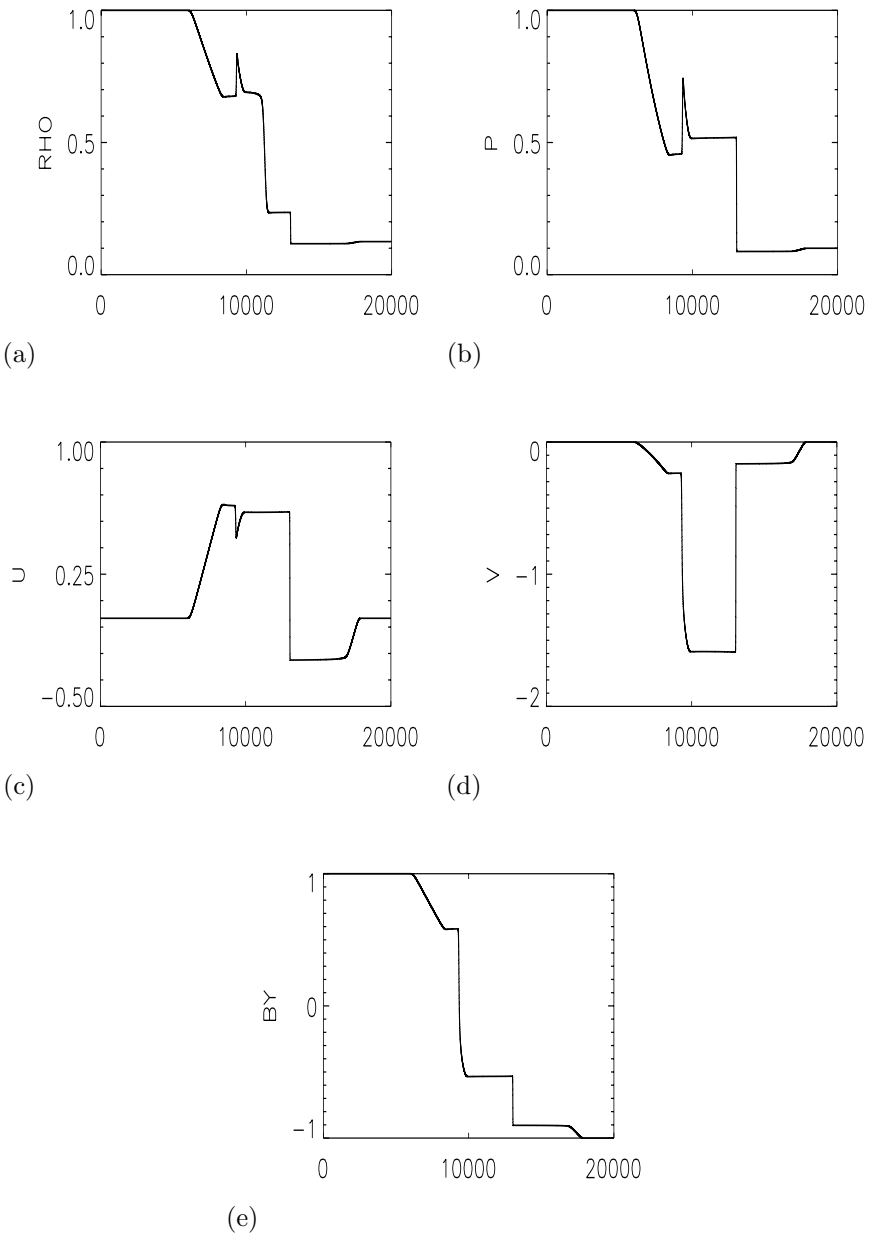


FIG. 6. *Lax–Friedrichs scheme for the Brio–Wu test problem with* $\gamma = 2$, 20,000 *cells, and* 40,000 *timesteps.*

We define $\tilde{\mathbf{U}}_i^* = (U_i^*(2), U_i^*(3), (U_i^*(4), U_i^*(5), U_i^*(6), U_i^*(7))^T$. Then from (3.4) and (5.1)

$$\tilde{\mathbf{U}}_L^* = \tilde{\mathbf{U}}^* - \alpha\sigma\Delta\tilde{\mathbf{U}},$$

where $1 > \sigma = (S_R - S_M)/(S_R - S_L) > 0$. Positive pressure in the left-star region

Downloaded 07/08/12 to 147.8.148.246. Redistribution subject to SIAM license or copyright; see http://www.siam.org/journals/ojsa.php

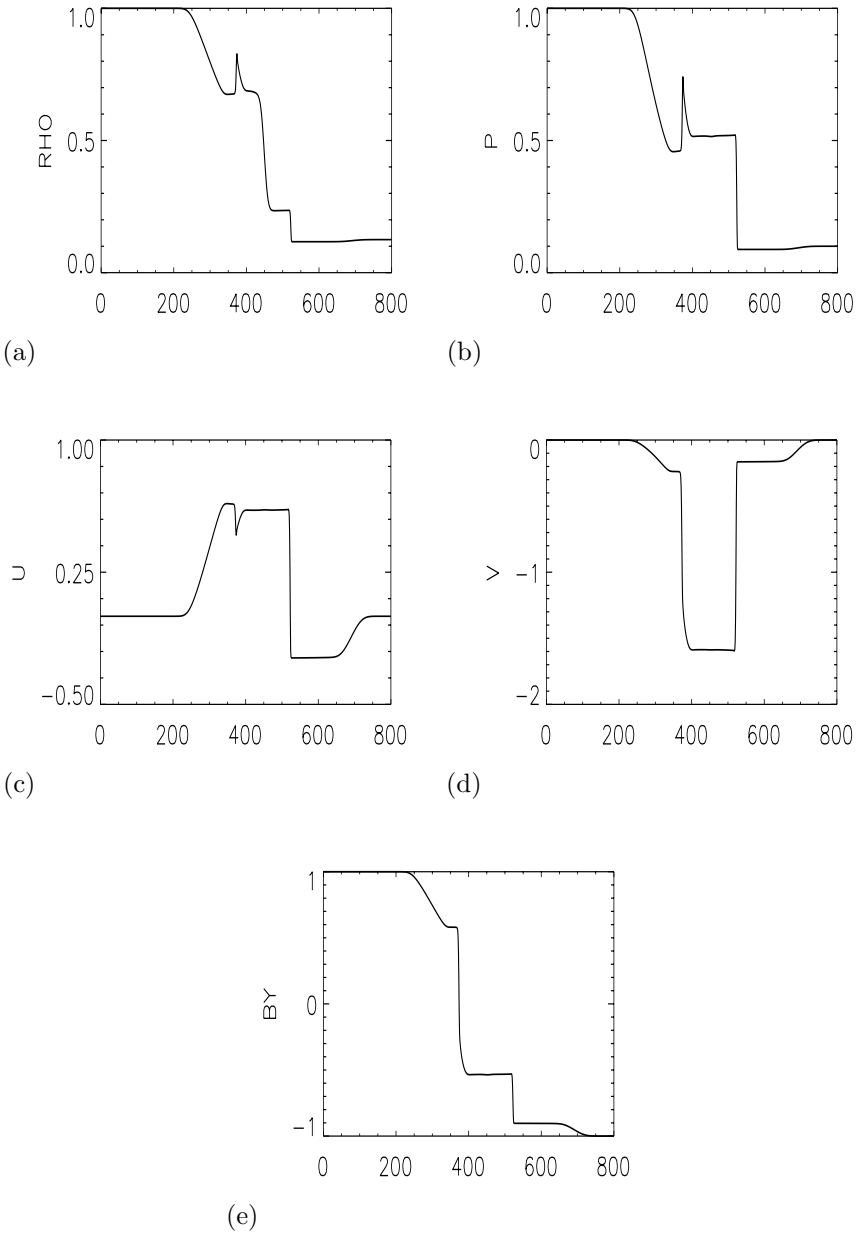


FIG. 7. *Smooth HLLC-MHD method results for the Brio–Wu* [3] *test problem with* $\gamma = 2$, $CFL = 0.8$, *and* 800 *cells.*

requires

$$e_L^* - \frac{\left(\left(\rho_L^* v_{nL}^*\right)^2 + \left(\rho_L^* v_{\tau_1 L}^*\right)^2 + \left(\rho_L^* v_{\tau_2 L}^*\right)^2\right)}{2\rho_L^*} + \frac{\left(B_n^2 + (B_{\tau_1 L}^*)^2 + (B_{\tau_2 L}^*)^2\right)}{8\pi} > 0 \qquad \text{or}$$

$$\alpha^2 C_2 - \alpha C_1 - C_0 < 0, \tag{6.12}$$

Downloaded 07/08/12 to 147.8.148.246. Redistribution subject to SIAM license or copyright; see http://www.siam.org/journals/ojsa.php

where

$$C_0 = 2\phi^*\rho_L^* + \mathbf{M}^{*2}\left(\frac{\rho_L^*}{\rho^*} - 1\right),$$
$$C_1 = 2\sigma\left(\rho_L^*\left(\frac{1}{4\pi}\mathbf{B}^*\cdot\Delta\mathbf{B} - \Delta e\right) + \mathbf{M}^*\cdot\Delta\mathbf{M}\right),$$
$$C_2 = \sigma^2\left(\Delta\mathbf{M}^2 + \frac{1}{4\pi}\rho_L^*\Delta\mathbf{B}^2\right),$$

where $\mathbf{M} = (\rho v_n, \rho v_{\tau_1}, \rho v_{\tau_2})$, $C_2 \geq 0$, and

$$\phi^* = e^* - \frac{\left(\left(\rho^* v_n^*\right)^2 + \left(\rho^* v_{\tau_1}^*\right)^2 + \left(\rho^* v_{\tau_2}^*\right)^2\right)}{2\rho^*} + \frac{\left(B_n^2 + B_{\tau_1}^* + B_{\tau_2}^*\right)}{8\pi} > 0.$$

We find that (6.12) cannot be satisfied for all $\alpha$ and $\sigma$. If we make changes to $\sigma$, then we will need to change $S_L$, $S_R$, and $S_M$, which also will require changes to the timesteps in the underlying Godunov method. However, we can easily make changes to $\alpha$ to preserve positivity without sacrificing our conditions that bound $S_L$ and $S_R$ by the exact expansion-wave velocities.

If $C_1 = C_2 = 0$, then the positivity of $\phi_L^*$ is independent of all choices of $\alpha$. If $C_0$ is not positive, then the method will test whether the HLL method gives positivity without varying the $S_R$ and $S_L$ wavespeeds. If the positivity of the HLL solver requires enlarging the Riemann fan, it may be beneficial to switch to another Riemann solver. However, $C_0$ always was positive when $C_1 = C_2 = 0$ in the numerical simulations conducted by the author.

Clearly if $C_2 = C_1 = 0$, $C_0 > 0$, then no additional restrictions are needed on $\alpha$. If $C_2 = 0$ and $C_1/C_0 > 0$, then (6.12) becomes $\alpha > -C_0/C_1 = \beta_L$, which is satisfied for any choice of nonnegative $\alpha$. If $C_2 = 0$ and $C_1/C_0 < 0$, then $\alpha > \beta_L > 0$ requires an additional restriction on $\alpha$. If $C_2$ is nonzero, then (6.12) becomes

$$\left(\alpha + \frac{C_1}{2C_2}\right)^2 < \frac{C_1^2 + 4C_0C_2}{4C_2^2},$$
$$\left|\alpha + \frac{C_1}{2C_2}\right| < \frac{\sqrt{C_1^2 + 4C_0C_2}}{2C_2}, \qquad \text{or}$$
$$\alpha < \frac{\sqrt{C_1^2 + 4C_0C_2}}{2C_2} + \left|\frac{C_1}{2C_2}\right|$$
$$\text{as} \quad \alpha \leq \left|\alpha + \frac{C_1}{2C_2}\right| + \left|\frac{C_1}{2C_2}\right| = \gamma_L.$$

Therefore, in summary, the subsequent conditions on $\alpha$ are as follows:

$$\text{(6.13)} \quad \begin{cases} \text{If} \quad C_1 = 0, \quad C_2 = 0, & \text{then} \quad \alpha_{pos} = \alpha, \quad \text{assuming} \quad C_0 > 0. \\ \text{If} \quad C_2 = 0, \quad C_1/C_0 > 0, & \text{then} \quad \alpha_{pos} = \alpha. \\ \text{If} \quad C_2 = 0, \quad C_1/C_0 < 0, & \text{then} \quad \alpha_{pos} = \max[\alpha, \beta_L]. \\ \text{If} \quad C_2 \neq 0, & \text{then} \quad \alpha_{pos} = \min[\alpha, \gamma_L]. \end{cases}$$

We have similar conditions on $\alpha$ from the right-hand intermediate pressure expression, $\phi_R^*$, to guarantee positivity. Note that unlike the HLLC method for gas dynamics and the unsmoothed MHD-HLLC method, there is only one possible, but unlikely, case ($C_2 = C_1 = 0$, $C_0 \leq 0$) where it is necessary to alter the wavespeeds of the Riemann fan for the underlying HLL method to guarantee positive pressures.

Downloaded 07/08/12 to 147.8.148.246. Redistribution subject to SIAM license or copyright; see http://www.siam.org/journals/ojsa.php

**7. Discussion.** In this paper we have presented an approximate Riemann solver for MHD based on the HLLC gas dynamics solver. The solver includes an algorithm to guarantee the positivity of pressure and density for almost all cases without altering the wavespeed of the outermost waves in the Riemann fan. Analytic results prove that the method exactly resolves isolated contact discontinuities and fast shock waves.

While the smoothed HLLC-MHD scheme can be considered a variant of Linde's "adequate" method, it has numerous advantages over Linde's scheme. First we must acknowledge the disadvantage that the formulation of the smoothed HLLC-MHD method is slightly more complex than Linde's scheme. However, the smoothed HLLC-MHD method benefits in having a well-defined middle wavespeed, $S_M$, based on the HLL method rather than a Roe-average, and a true scalar definition for the smoothing constant, $\alpha$. The extra computations needed to define $S_M$ and $\alpha$ over the computations needed for Linde's method are still very small compared to the number of computations necessary for either a nonlinear or Roe solver. In addition, the smooth HLLC-MHD method provides a means to control positivity, a measure lacking in Linde's scheme. We have not shown numerical comparisons between the smooth HLLC-MHD method and Linde's scheme for the Ryu–Jones and Brio–Wu one-dimensional test problems shown because the results are, as expected, nearly indistinguishable when the same method for defining Roe-averages is used. Preliminary results indicate that the two methods give different results in multidimensional problems, a subject that will be discussed in a future paper.

**Acknowledgments.** The author wishes to thank P. Colella, D. S. Spicer, and S. T. Zalesak for many valuable discussions.

REFERENCES

[1] D. S. Balsara, *Total variation diminishing scheme for adiabatic and isothermal magnetohydrodynamics*, Astrophys. J. Supplement Series, 116 (1998), pp. 144–153.

[2] P. Batten, N. Clarke, C. Lambert, and D. M. Causon, *On the choice of wavespeeds for the HLLC Riemann solver*, SIAM J. Sci. Comput., 18 (1997), pp. 1553–1570.

[3] M. Brio and C. Wu, *An upwind differencing scheme for the equations of ideal magnetohydrodynamics*, J. Comput. Phys., 75 (1988), pp. 400–422.

[4] P. Cargo and G. Gallice, *Roe matrices for ideal MHD and systematic construction of Roe matrices for systems of conservation laws*, J. Comput. Phys., 136 (1997), pp. 446–466.

[5] S. F. Davis, *Simplified second-order Godunov-type methods*, SIAM J. Sci. Statist. Comput., 9 (1988), pp. 445–473.

[6] B. Einfeldt, *On Godunov-type methods for gas dynamics*, SIAM J. Numer. Anal., 25 (1988), pp. 294–318.

[7] B. Einfeldt, C. D. Munz, P. L. Roe, and B. Sjögreen, *On Godunov-type methods near low densities*, J. Comput. Phys., 92 (1991), pp. 273–295.

[8] K. O. Friedrichs and H. Kranzer, *Notes on Magneto-hydrodynamics,* VII. *Nonlinear Wave Motion*, Tech. Report NYO-6486-VII, Courant Institute of Mathematical Sciences, Magneto-Fluid Dynamics Division, New York University, New York, 1958.

[9] S. K. Godunov, *A difference method for the numerical calculation of discontinuous solutions of hydrodynamic equations*, Mat. Sb., 47 (1959).

[10] T. I. Gombosi, D. L. DeZeeuw, R. M. Häberlin, and K. G. Powell, *Three-dimensional multiscale MHD model of cometary plasma environments*, J. Geophys. Res., 101 (1996), pp. 15233–15253.

[11] A. Harten, P. D. Lax, and B. van Leer, *On upstream differencing and Godunov-type schemes for hyperbolic conservation laws*, SIAM Rev., 25 (1983), pp. 35–61.

[12] P. Janhunen, *A positive conservative method for magnetohydrodynamics based on HLL and Roe methods*, J. Comput. Phys., 160 (2000), pp. 649–661.

[13] T. J. Linde, *A Three-Dimensional Adaptive Multifluid MHD Model of the Heliosphere*, Ph.D. Dissertation, University of Michigan, Ann Arbor, MI, 1998.

[14] T. J. Linde, T. I. Gombosi, P. L. Roe, K. G. Powell, and D. L. DeZeeuw, *The heliosphere in magnetized local interstellar medium: Results of a 3D MHD simulation*, J. Geophys. Res., 103 (1998), pp. 1889–1904.

[15] K. G. Powell, *An Approximate Riemann Solver for Magnetohydrodynamics (That Works in More than One Dimension)*, Tech. Report 94-24, ICASE, NASA Langley Research Center, Hampton, VA, 1994.

[16] K. G. Powell, P. L. Roe, T. J. Linde, T. I. Gombosi, and D. L. DeZeeuw, *A solution-adaptive upwind scheme for ideal magnetohydrodynamics*, J. Comput. Phys., 154 (1999), pp. 284–309.

[17] P. L. Roe, *Approximate Riemann solvers, parameter vectors and difference schemes*, J. Comput. Phys., 43 (1981), pp. 357–372.

[18] D. Ryu and T. W. Jones, *Numerical magnetohydrodynamics in astrophysics: Algorithm and tests for one-dimensional flow*, Astrophys. J., 442 (1995), pp. 228–258.

[19] T. Tanaka, *Finite volume TVD scheme on an unstructured grid system for three-dimensional MHD simulations of inhomogeneous systems including strong background potential field*, J. Comput. Phys., 111 (1994), pp. 381–389.

[20] E. F. Toro, *Riemann Solvers and Numerical Methods for Fluid Dynamics*, Springer-Verlag, Berlin, 1999.

[21] E. F. Toro, M. Spruce, and W. Speares, *Restoration of the contact surface in the HLL-Riemann solver*, Shock Waves, 4 (1994), pp. 25–34.

[22] A. L. Zachary and P. Colella, *A higher-order Godunov method for the equations of ideal magnetohydrodynamics*, J. Comput. Phys., 99 (1992), pp. 341–347.

Downloaded 07/08/12 to 147.8.148.246. Redistribution subject to SIAM license or copyright; see http://www.siam.org/journals/ojsa.php